Sparse Polynomial Chaos Expansions: Solvers, Basis Adaptivity and Meta-selection

Nora Lüthen, Stefano Marelli, Bruno Sudret

ETH zürich

Sparse Polynomial Chaos Expansions: Solvers, Basis Adaptivity and Meta-selection

N. Lüthen, S. Marelli and B. Sudret

Chair of Risk, Safety and Uncertainty Quantification
Stefano-Franscini-Platz 5
CH-8093 Zürich

Risk, Safety & Uncertainty Quantification

Data Sheet

Journal:	-
Report Ref.:	RSUQ-2020-011
Arxiv Ref.:	https://arxiv.org/abs/2009.04800 [cs.NA, stat.CO, stat.ML]
DOI:	-
Date submitted:	September 10, 2020
Date accepted:	-

Sparse Polynomial Chaos Expansions: Solvers, Basis Adaptivity and Meta-selection

Nora Lüthen[1], Stefano Marelli[1], and Bruno Sudret[1]

[1] *Chair of Risk, Safety and Uncertainty Quantification, ETH Zürich, Stefano-Franscini-Platz 5, 8093 Zürich, Switzerland*

September 10, 2020

Abstract

Sparse polynomial chaos expansions (PCEs) are an efficient and widely used surrogate modeling method in uncertainty quantification. Among the many contributions aiming at computing an accurate sparse PCE while using as few model evaluations as possible, basis adaptivity is a particularly interesting approach. It consists in starting from an expansion with a small number of polynomial terms, and then parsimoniously adding and removing basis functions in an iterative fashion. We describe several state-of-the-art approaches from the recent literature and extensively benchmark them on a large set of computational models representative of a wide range of engineering problems. We investigate the synergies between sparse regression solvers and basis adaptivity schemes, and provide recommendations on which of them are most promising for specific classes of problems. Furthermore, we explore the performance of a novel cross-validation-based solver and basis adaptivity selection scheme, which consistently provides close-to-optimal results.

1 Introduction

Surrogate modeling techniques are a popular tool in applied sciences and engineering, because they can significantly reduce the computational cost of uncertainty quantification analysis for costly real-world computational models. Here, the computational model is approximated by a cheaper-to-evaluate function, which is created based on a small number of model evaluations, the so-called experimental design. One well-known and popular surrogate modeling technique is polynomial chaos expansion (PCE), which approximates the output of a computational model by a spectral expansion in terms of an orthonormal polynomial basis in the input random variables (Xiu and Karniadakis, 2002). PCE is particularly well suited for surrogating smooth models in low to medium dimension, and for the efficient computation of moments and Sobol' indices (Sudret, 2008; Le Gratiet et al., 2017). Sparse PCE techniques, which aim to compute an expansion involving only few terms, have proven especially powerful and cost-efficient for real-world engineering problems such as, among many others, surrogate-assisted robust design

optimization (Chatterjee et al., 2019), hybrid simulation for earthquake engineering (Abbiati et al., 2021), dam engineering (Guo et al., 2019; Harari-Ardebili and Sudret, 2020), and wind turbine design (Slot et al., 2020).

In the last decade, a large amount of literature on sparse PCE has been published, proposing methods that make sparse PCE more accurate, efficient and applicable to high-dimensional problems. However, it is often not obvious how well these methods perform when compared to and combined with each other, especially on real-world engineering problems. In an attempt to fill this gap, the authors recently conducted a literature survey on sparse PCE and a classification of the available methods into a general framework, as well as a benchmark of selected methods on a broad class of computational models (Lüthen et al., 2020). This benchmark extensively compared sparse regression solvers and experimental design sampling schemes, using a fixed truncation scheme for the polynomial basis.

The goal of the present paper is to complement this benchmark by exploring the promising field of *basis-adaptive sparse PCE*, in which the basis is iteratively augmented and refined. We describe several basis-adaptive schemes from the sparse PCE literature in detail, namely, degree and q-norm adaptivity (Blatman and Sudret, 2011; Marelli and Sudret, 2019), forward neighbor degree adaptivity (Jakeman et al., 2015), and anisotropic degree basis adaptivity (Hampton and Doostan, 2018). The performance and synergies of combinations of sparse regression solvers and basis adaptivity schemes are then evaluated in terms of validation error on a library of 11 computational models of varying complexity, representative of a broad class of engineering models. These range from three- to 100-dimensional and include both analytical and numerical models. Furthermore, we explore the idea of performing an additional selection of sparse PCEs among several candidate PCEs computed by different combinations of methods on the same experimental design, using a cross-validation estimate for the generalization error.

The paper is structured as follows. In Section 2, we recall the definition of (sparse) PCE and the computing framework introduced by Lüthen et al. (2020). We discuss various estimators for the generalization error, sparse regression solvers, and basis adaptivity, and introduce meta-selection. The associated benchmark results for basis adaptivity and meta-selection are presented in Section 3. Finally, a discussion and summary of our results is provided in Section 4. Additional information and results can be found in the Appendix.

2 Sparse polynomial chaos expansions

Let $\boldsymbol{X}$ be a d-dimensional random vector with mutually independent components and probability density function $f_{\boldsymbol{X}}$. Denote by $\mathcal{D}_{\boldsymbol{X}}$ the domain of the random vector $\boldsymbol{X}$. Define the space $L^2_{f_{\boldsymbol{X}}}(\mathcal{D}_{\boldsymbol{X}}) = \{h : \mathcal{D}_{\boldsymbol{X}} \to \mathbb{R} \mid \mathrm{Var}_{\boldsymbol{X}}[h(\boldsymbol{X})] < +\infty\}$ of all scalar valued models with finite variance under $f_{\boldsymbol{X}}$. Under very general conditions on the input distribution $f_{\boldsymbol{X}}$, there exists a polynomial basis $\{\psi_{\boldsymbol{\alpha}} : \boldsymbol{\alpha} \in \mathbb{N}^d\}$ of $L^2_{f_{\boldsymbol{X}}}(\mathcal{D}_{\boldsymbol{X}})$ (Xiu and Karniadakis, 2002; Ernst et al., 2012). Since the components of $\boldsymbol{X}$ are mutually independent, each polynomial basis function can be built as a product of univariate polynomials in $X_1, \ldots, X_d$ and characterized by the multi-index $\boldsymbol{\alpha} \in \mathbb{N}^d$

whose entries are equal to the degrees of the univariate terms.

For a computational model $\mathcal{M} \in L^2_{f_{\boldsymbol{X}}}(\mathcal{D}_{\boldsymbol{X}})$, let $Y = \mathcal{M}(\boldsymbol{X})$ denote the output random variable. Y can be cast as the following spectral expansion:

$$Y = \mathcal{M}(\boldsymbol{X}) = \sum_{\boldsymbol{\alpha} \in \mathbb{N}^d} c_{\boldsymbol{\alpha}} \psi_{\boldsymbol{\alpha}}(\boldsymbol{X}). \tag{1}$$

In practice, a finite, *truncated polynomial chaos expansion*

$$Y = \mathcal{M}(\boldsymbol{X}) \approx \mathcal{M}^{\mathrm{PCE}}(\boldsymbol{X}) = \sum_{\boldsymbol{\alpha} \in \mathcal{A}} c_{\boldsymbol{\alpha}} \psi_{\boldsymbol{\alpha}}(\boldsymbol{X}) \tag{2}$$

is computed, where $\mathcal{A} \subset \mathbb{N}^d$ is the truncation set defining the basis elements used in the expansion. The accuracy of the expansion depends on $\mathcal{A}$ and the coefficient values $(c_{\boldsymbol{\alpha}})_{\boldsymbol{\alpha} \in \mathcal{A}} =: \boldsymbol{c} \in \mathbb{R}^P$, with $P = \mathrm{card}(\mathcal{A})$.

Among several methods for computing the coefficient vector $\boldsymbol{c}$ for a given truncation set, *sparse regression* is a particularly powerful and efficient method (Doostan and Owhadi, 2011; Blatman and Sudret, 2011). In this approach, the model is evaluated at a number of points $\boldsymbol{\mathcal{X}} = \{\boldsymbol{x}^{(1)}, \ldots, \boldsymbol{x}^{(N)}\} \subset \mathcal{D}_{\boldsymbol{X}}$ called the *experimental design* (ED), yielding the vector of model responses $\boldsymbol{y} = (\mathcal{M}(\boldsymbol{x}^{(1)}), \ldots, \mathcal{M}(\boldsymbol{x}^{(N)}))^T$. Let $\{\boldsymbol{\alpha}_j\}_{j=1}^P$ be an arbitrary ordering of the multi-indices in the truncation set and define the regression matrix $\boldsymbol{\Psi} \in \mathbb{R}^{N \times P}$ with entries $\Psi_{ij} = \psi_{\boldsymbol{\alpha}_j}(\boldsymbol{x}^{(i)})$. Sparse regression methods determine a vector $\boldsymbol{c}$ that minimizes the residual norm $\|\boldsymbol{\Psi c} - \boldsymbol{y}\|_2$ under the constraint that it has only few nonzero entries i.e., it is *sparse*. This is usually achieved by regularized regression, resulting e.g. in the LASSO formulation

$$\hat{\boldsymbol{c}} = \min_{\boldsymbol{c} \in \mathbb{R}^P} \|\boldsymbol{\Psi c} - \boldsymbol{y}\|_2^2 \quad \text{s.t.} \quad \|\boldsymbol{c}\|_1 \leq \tau, \tag{3}$$

where τ is a parameter regulating the sparsity of $\boldsymbol{c}$. A PCE with a sparse coefficient vector $\boldsymbol{c}$ is called *sparse PCE*. Provided that the regression matrix fulfills certain properties (Candès and Wakin, 2008; Bruckstein et al., 2009; Candès and Plan, 2011), sparse regression can find robust solutions to underdetermined systems of linear equations, which means that the experimental design can be smaller than the number of unknown coefficients.

The quality of the solution depends on the choice of the basis $\mathcal{A}$, on the experimental design $\boldsymbol{\mathcal{X}}$, and on the method used for computing the coefficients. For each of these components, many different methods have been proposed in recent years, including iterative methods which adaptively determine $\mathcal{A}$, or the experimental design $\boldsymbol{\mathcal{X}}$. These methods were recently surveyed and classified into the framework shown in Fig. 1 (modified from Lüthen et al. (2020)). In the present contribution, we focus on the question of how to determine a suitable basis $\mathcal{A}$. To this end, we benchmark several basis-adaptive approaches and explore their interplay with sparse regression solvers.

2.1 Error estimation and model selection

Model selection is applied on several levels in the sparse PCE framework:

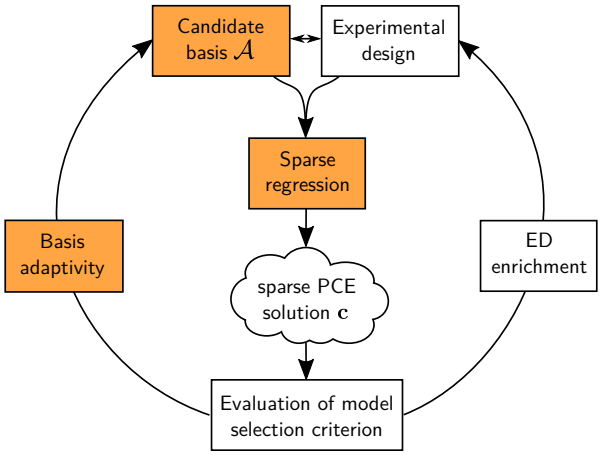

Figure 1: *Framework for computing sparse PCE introduced by Lüthen et al. (2020), who conducted a literature survey and a benchmark for the central components "Experimental design" and "Sparse regression" (adapted from Lüthen et al. (2020)). In the present work, we discuss and benchmark the components marked in orange. In particular, we discuss the component "Basis adaptivity" and explore its relationship to sparse regression solvers.*

- Within the sparse solver to select its hyperparameter (see Section 2.2)
- Within the basis adaptivity scheme to select a basis (see Section 2.3)
- Finally, between solvers and basis adaptivity schemes, to automatically select a combination that is close to best (see Section 2.4).

Our main quantity of interest is the generalization error, in the form of the relative mean squared error normalized by the model variance

$$E_{\text{gen}} = \frac{\mathbb{E}_{\boldsymbol{X}}\left[(\mathcal{M}(\boldsymbol{X}) - \mathcal{M}^{\text{PCE}}(\boldsymbol{X}))^2\right]}{\text{Var}_{\boldsymbol{X}}\left[\mathcal{M}(\boldsymbol{X})\right]}. \tag{4}$$

It can be approximated by the validation error in the form of the relative mean squared error (MSE)

$$\text{RelMSE} = \frac{\sum_{i=1}^{N_{\text{val}}}\left(\mathcal{M}(\boldsymbol{x}_{\text{val}}^{(i)}) - \mathcal{M}^{\text{PCE}}(\boldsymbol{x}_{\text{val}}^{(i)})\right)^2}{\sum_{i=1}^{N_{\text{val}}}\left(\mathcal{M}(\boldsymbol{x}_{\text{val}}^{(i)}) - \frac{1}{N_{\text{val}}}\sum_{j=1}^{N_{\text{val}}}\mathcal{M}(\boldsymbol{x}_{\text{val}}^{(j)})\right)^2} \tag{5}$$

computed on a large validation set $\{\boldsymbol{x}_{\text{val}}^{(i)}\}_{i=1}^{N_{\text{val}}} \sim_{\text{i.i.d.}} f_{\boldsymbol{X}}$. We only consider model selection criteria that are estimates of the generalization error.

To get an accurate estimate of the generalization error, without using an additional validation set, a widely used method is *cross-validation* (Vapnik, 1995). Here, the available data is repeatedly divided into two disjoint sets, one for computing the solution (training) and the other for evaluating the error (validation). Aggregating the error estimates from the different splits, we get a cross-validation estimate of the generalization error.

One cross-validation strategy is to divide the data randomly into k disjoint, roughly equally large parts, and use each of the parts in turn as validation set. This is called *k-fold cross-validation.*

If k is chosen to be equal to the size of the experimental design, the strategy is known as *leave-one-out cross-validation* (LOO). This is closest to using all data points to compute a solution, since in each iteration, only one point is left out from the training set.

In general, LOO can be quite costly, since for an experimental design of size N, the method under consideration has to be applied N times. A cheap approximation to the LOO error, which requires only one application of the method, is available for certain sparse regression solvers, namely for those which in their last step recompute the solution with ordinary least-squares (OLS) on the set of regressors with nonzero coefficient (called *active basis*) (Blatman and Sudret, 2010a). In particular, this is the case for the solvers hybrid least angle regression (LARS) (Blatman and Sudret, 2011), orthogonal matching pursuit (OMP) (Pati et al., 1993; Jakeman et al., 2015), and subspace pursuit (SP) (Diaz et al., 2018) (see Section 2.2). For these solvers, the OLS-based LOO estimate coincides with the true LOO error if the following holds: regardless of which experimental design point is left out, the sparse regression solver consistently yields the same active basis.

Since the repeated use of LOO for model selection often results in the generalization error being underestimated, especially on small experimental designs, Blatman and Sudret (2011) proposed to use a modification factor originally developed for the empirical error (Chapelle et al., 2002), defined by

$$T = \frac{N}{N - P_{\text{active}}} \left(1 + \text{tr}((\mathbf{\Psi}_{\text{active}}^T \mathbf{\Psi}_{\text{active}})^{-1})\right), \tag{6}$$

where P_{active} denotes the number of nonzero coefficients (the corresponding basis functions are called *active*), and $\mathbf{\Psi}_{\text{active}}$ denotes the regression matrix containing only the active regressors. The product of the modification factor T with the LOO error is called *modified LOO error*.

2.2 Sparse regression solvers

Various sparse regression solvers available for solving sparse PCE were described in detail by Lüthen et al. (2020). We give here only a short overview of the solvers used in our benchmark, and refer to Lüthen et al. (2020) for further details. These solvers are common choices in the sparse PCE literature.

- Hybrid least angle regression (LARS) (Blatman and Sudret, 2011): adding regressors one-by-one, following a least-angle strategy. The hybrid approach recomputes the final coefficient values by ordinary least squares (OLS) on the selected regressors.
- Orthogonal matching pursuit (OMP) (Pati et al., 1993; Jakeman et al., 2015): greedily adding orthogonal regressors one-by-one, computing their coefficients by OLS.
- Subspace pursuit (SP) (Diaz et al., 2018): searching iteratively for a solution with a certain ℓ^0-norm by adding and removing regressors from the active set. Coefficients are computed by OLS. We include two variants of SP in this benchmark, one which determines its hyperparameter by 4-fold cross-validation as implemented by Diaz (2018), which we

denote by $\mathrm{SP}_{k=4}$, and one where it is determined by OLS-based LOO, introduced in Lüthen et al. (2020) and denoted by $\mathrm{SP}_{\mathrm{LOO}}$.

- Bayesian compressive sensing (BCS) (Babacan et al., 2010): using a Bayesian framework to enforce sparsity of the coefficients.
- SPGL1 (van den Berg and Friedlander, 2008): a convex optimization solver following the Pareto front of the residual-sparsity trade-off.

Each of the solvers features at least one hyperparameter whose value needs to be determined via cross-validation in order to get a good solution. For LARS, OMP, $\mathrm{SP}_{k=4}$, and $\mathrm{SP}_{\mathrm{LOO}}$, this hyperparameter is the number of active basis functions (nonzero coefficients) of the final solution. For BCS and SPGL1, it is the bound on the residual norm in the sparse regression formulation.

The benchmark by Lüthen et al. (2020) of sparse regression solvers on a non-adaptive polynomial basis showed that BCS and $\mathrm{SP}_{\mathrm{LOO}}$ generally outperform other sparse solvers for low-dimensional models, while for high-dimensional models, BCS is by far the best sparse solver.

2.3 Basis adaptivity

The sparse solver and the experimental design, which were benchmarked in Lüthen et al. (2020), are not the only ingredients to a sparse PCE. The choice of the *candidate basis*, from which the sparse solver determines the *active basis* (i.e., the set of regressors with nonzero coefficient), is another important ingredient: if the candidate basis is chosen too small, important terms might be missing, which might lead to a large model error. On the other hand, if the candidate basis is too large, the ratio of the number of experimental design points to the number of coefficients is small, which causes some properties of the regression matrix to deteriorate and can result in a large approximation error.

Of course, it is not possible to know a-priori the best choice of the candidate basis. Basis-adaptive schemes start with an initial candidate basis and adapt it iteratively, adding or removing basis functions in each iteration according to various heuristics. The performance of the bases in the different iterations is evaluated using a model selection criterion, typically an estimate of the generalization error.

Several procedures for basis-adaptive sparse PCE have been proposed in the literature. We discuss three approaches in detail, namely

- degree and q-norm ("p&q") basis adaptivity, as implemented in UQLab (Marelli and Sudret, 2019), see Section 2.3.1;
- forward neighbor basis adaptivity (Jakeman et al., 2015), see Section 2.3.2; and
- anisotropic degree basis adaptivity (Hampton and Doostan, 2018), from the software BASE_PC (Hampton and Doostan, 2017), see Section 2.3.3.

We also briefly mention several other approaches found in the literature.

2.3.1 Degree and q-norm ("p&q") adaptivity

A typical choice for a PCE basis is the *basis of total degree p* defined by the set of multi-indices

$$\mathcal{A}^p = \{\boldsymbol{\alpha} \in \mathbb{N}^d : \sum_{i=1}^{d} \alpha_i \leq p\}. \tag{7}$$

Furthermore, *hyperbolic truncation* (Blatman and Sudret, 2011) uses the q-(quasi-)norm

$$\|\boldsymbol{x}\|_q = \left(\sum_{i=1}^{d} |x_i|^q\right)^{\frac{1}{q}} \tag{8}$$

with $q \in (0, 1]$ to truncate a total-degree basis further:

$$\mathcal{A}^{p,q} = \{\boldsymbol{\alpha} \in \mathbb{N}^d : \|\boldsymbol{\alpha}\|_q \leq p\}. \tag{9}$$

Hyperbolic truncation has the effect of excluding some of the basis functions with high degree and high interaction order. This is particularly effective for high-dimensional problems.

A simple basis-adaptive scheme is *degree adaptivity* (Blatman and Sudret, 2011), which computes a number of PCEs on a sequence of total-degree candidate bases of increasing size, and returns the PCE minimizing a certain error estimate as final solution. Analogously, a q-norm adaptive scheme can be developed, and easily be combined with degree adaptivity (Marelli and Sudret, 2019), yielding *degree and q-norm (p&q) adaptivity*. Degree and q-norm adaptivity is solution-agnostic, i.e., it does not take the solution computed in the previous iteration into account.

2.3.2 Forward neighbor basis adaptivity

Jakeman et al. (2015) suggest a basis-adaptive algorithm based on a graph view of the PCE regressors (see also Gerstner and Griebel (2003); Narayan and Jakeman (2014)).

Since the input random vector is assumed to have independent components, the basis functions have tensor product structure. The basis functions can be considered nodes of a directed acyclic graph constructed as follows: two regressors are considered neighbors if their multi-index of degrees differs only in one dimension by 1, i.e., there is a directed edge from $\psi_{\boldsymbol{\alpha}}$ to $\psi_{\boldsymbol{\beta}}$ iff $\boldsymbol{\gamma} := \boldsymbol{\beta} - \boldsymbol{\alpha}$ is a multi-index with $\gamma_i = 1$ for one $i \in \{1, \ldots, d\}$ and $\gamma_j = 0, j \neq i$. *Forward neighbors* of a regressor are regressors reachable by an outgoing edge, and *backwards neighbors* are regressors connected by an incoming edge.

In the context of basis-adaptive PCE, this construction is used to determine a number of candidate regressors to be added to the currently active basis, starting from an initial basis of small total degree. Assume that an important high-degree or high-order regressor is not yet part of the candidate basis but some of its backwards neighbors are. The fact that it is missing should be visible in the coefficients of its backwards neighbors, which can be expected to have a significant nonzero coefficient to compensate for the fact that the important high-degree regressor is not yet part of the basis.

This heuristic is the foundation of the algorithm whose pseudocode is summarized in Algorithm 1. In each iteration, the current set of active basis functions is determined (restriction step). All forward neighbors of these active basis functions are surveyed and added to the candidate basis if they are *admissible*, i.e., if all of their backwards neighbors are in the active set (expansion step). Jakeman et al. (2015) employ several expansion steps to prevent premature termination, and use cross-validation error estimates. We call this algorithm *forward neighbor basis-adaptive*.

Algorithm 1 Forward neighbor basis adaptivity (Jakeman et al., 2015)

1: Initial PCE (basis chosen a-priori, typically small total-degree basis)
2: Restriction: retain only the active regressors $\mathcal{A}^{\text{active}}$
3: Expansion: let $\mathcal{A}^{(0)} = \mathcal{A}^{\text{active}}$. For $t = 1, \ldots, T$, obtain the set $\mathcal{A}^{(t)}$ by augmenting $\mathcal{A}^{(t-1)}$ by all its admissible forward neighbors.
4: Compute a PCE and its error estimate for each augmented basis $\mathcal{A}^{(1)}, \ldots, \mathcal{A}^{(T)}$.
5: Choose the PCE with the lowest error estimate among the T candidates. Stop if this error estimate is larger than the previously obtained best error estimate. Else, continue iteration with restriction step (Step 2)

This algorithm is implemented in the software Dakota (Adams et al., 2014). We use our own Matlab-based implementation of the algorithm. Consistently with (Jakeman et al., 2015), we set $T = 3$.

2.3.3 Anisotropic degree basis adaptivity

Hampton and Doostan (2018) propose an algorithm called BASE-PC, which combines a basis-adaptive scheme with sequential enrichment of a coherence-optimal experimental design. The two steps are executed alternatingly: based on the current ED, a suitable basis is chosen; and according to the currently active basis functions, the ED is enriched and the weights are updated.

In the present work, we solely consider the basis adaptivity part of the BASE-PC algorithm. The main idea of this algorithm is to use an *anisotropic degree basis*, defined by a *degree vector* $\boldsymbol{p} \in \mathbb{N}^d$. A related idea was explored earlier by Blatman and Sudret (2009). Similarly to a total-order basis, an anisotropic degree basis is defined by

$$\mathcal{A}^{\boldsymbol{p}} = \{\boldsymbol{\alpha} \in \mathbb{N}^d : \sum_{i=1}^{d} \frac{\alpha_i}{p_i} \leq 1\}. \tag{10}$$

If all entries of $\boldsymbol{p}$ are the same, i.e., $p_1 = p_2 = \ldots = p_d = p$, this definition reduces to a total-order basis of degree p. The equation $\sum_{i=1}^{d} \frac{\alpha_i}{p_i} = 1$ defines a hyperplane that cuts the i-th coordinate axis at $\alpha_i = p_i$.

In each iteration, the algorithm determines the current anisotropic degree vector based on the currently active basis. A new, larger candidate basis is then constructed by considering the anisotropic degree basis corresponding to a uniformly increased anisotropic degree vector.

We use our own, slightly modified implementation of the basis adaptivity part of BASE-PC, as summarized in Algorithm 2. The most costly operation is the computation of the anisotropic-degree basis (line 6). Hampton and Doostan (2018) developed a specialized efficient algorithm to generate the multi-indices of an anisotropic degree basis, which we utilize in our implementation. We call Algorithm 2 *anisotropic degree basis-adaptive*.

Algorithm 2 Anisotropic degree basis adaptivity (Hampton and Doostan, 2018)

1: Initial PCE (fixed basis of low order)
2: **for** $o = 1, \ldots, 10$ **do** ▷ outer loop
3: Restriction: denote by $\mathcal{A}^{\text{active}}$ the set of active regressors of the last selected PCE
4: **for** $i = 1, \ldots, 10$ **do** ▷ inner loop
5: Additional restriction: remove $\frac{i-1}{10}$ regressors from the set $\mathcal{A}^{\text{active}}$ starting with the ones with smallest-in-magnitude coefficients, obtaining a set $\mathcal{A}^i \subseteq \mathcal{A}^{\text{active}}$
6: Expansion: compute the dimension-wise maximal degree of the regressors in $\mathcal{A}^i$, denoted by degree vector $\boldsymbol{p}^{\max}$. Compute $\boldsymbol{p}^{\text{new}} = (p_1^{\max} + 1, p_2^{\max} + 1, \ldots, p_d^{\max} + 1)$ and the associated anisotropic-degree basis $\mathcal{A}^{i,\text{new}}$
7: Compute a PCE on the basis $\mathcal{A}^{i,\text{new}}$ and its error estimator e^i
8: If $e^i \geq e^{i-1}$, increase the so-called *strike counter* by 1. Break from the inner loop if the strike counter is ≥ 3
9: **end for**
10: From the 10 candidate PCEs, select the PCE with the lowest error estimate
11: Break from the outer loop if the error estimate has increased three times in subsequent iterations (ExpansionEarlyStop; same idea as inner loop strike counter)
12: **end for**
13: Return the PCE with the lowest error estimate among all PCEs selected in the outer loop.

2.3.4 Other basis adaptivity algorithms

We briefly summarize other approaches for basis adaptivity for sparse PCE. These approaches will not be investigated in our benchmark.

Many algorithms which use stepwise regression to build up a sparse basis regressor-by-regressor can be classified both as sparse regression solvers (as done in Lüthen et al. (2020)) and as basis-adaptive algorithms. As an example, the approach by Blatman and Sudret (2010a) adds and removes regressors one-by-one based on the induced change in LOO error, thereby building up a small set of active basis functions which is sparse in a larger total-degree basis. In this case, the candidate basis coincides with the active basis. Mai and Sudret (2015) use the "principle of heredity" together with LARS to determine additional bivariate interaction terms to be added to the model, once a univariate term is identified as relevant. We do not consider these approaches, since we are interested in algorithms modifying the candidate basis not only one regressor at a time, but at a larger scale.

Alemazkoor and Meidani (2017) propose a basis-adaptive algorithm relying on sparsity and step-

by-step augmentation of the basis. In each step, the candidate basis is a total-order basis for a subset of input random variables, while the remaining input random variables are considered constant. The initial basis consists only of the constant term. In each iteration, either one of the constant dimensions is activated, or the total degree of the candidate basis is increased by one (active dimensions only), depending on the resulting error estimate or sparsity of the solution. The coefficients are solved by OLS until a pre-defined threshold of residual norm is reached. Then, the sparse regression solver SPGL1 is used, which identifies the sparsest solution whose residual norm is smaller than the given threshold. We do not consider this method due to its high computational cost and its strong tie to the solver SPGL1, making it less effective when paired with other sparse regression solvers.

Loukrezis and De Gersem (2019) propose a basis-adaptive algorithm for interpolating PCE on Leja-based sparse grids. Their algorithm is a more cautious version of forward neighbor basis adaptivity (Section 2.3.2): after adding all admissible forward neighbors to the basis and computing their coefficients, all of the recently added regressors are removed again, except for the one that achieved the largest-in-magnitude coefficient. Thapa et al. (2020) suggest a basis-adaptive procedure that relies on total-order bases of increasing degree. In contrast with degree adaptivity (Section 2.3.1), the basis functions of degree $p+1$ are not added all at once, but in chunks of a certain size dependent on the dimension and the degree p. After adding a chunk of basis functions, the PCE is recomputed and regressors with a coefficient smaller than a certain threshold are removed from the basis. We do not consider these two approaches because they are similar to the previously presented approaches while being more costly.

2.4 Post-processing: selection of a sparse PCE solution from several candidate solutions

For realistic simulators used in engineering and applied sciences, evaluating the computational model is the expensive part of the surrogate modeling process. Once the model evaluations are obtained, all further computations are post-processing steps, and are computationally cheap in comparison to the model evaluations. Thus, it is feasible to apply several adaptive sparse PCE methods and choose the best one.

We therefore propose the use of an additional layer of selection (*meta-selection*, also known as *bagging* or *ensemble modeling*). For a given experimental design, we compute several sparse PCEs through different combinations of sparse solvers and basis adaptivity schemes. From the resulting PCE solutions, we choose one based on the value of a suitable estimate of generalization error as model selection criterion. There are several possibilities. One possible choice is the estimator already used for selecting the hyperparameter of the solver and for basis adaptivity, i.e., (modified) LOO for LARS, OMP and $\mathrm{SP}_{\mathrm{LOO}}$, and k-fold cross-validation for $\mathrm{SP}_{k=4}$, BCS and SPGL1. However, this estimator might not be consistent between solvers, which is however necessary for such a meta-selection. Furthermore, this estimate might be biased due to its repeated use.

A second class of estimators is given by the so-called *hybrid cross-validation error estimators*.

The word *hybrid* is a reference to Efron et al. (2004), who created the hybrid version of least-angle regression (LARS) which uses LARS only to identify the set of active basis functions, and then recomputes the coefficients by ordinary least-squares (OLS) on this active set. To compute the hybrid leave-one-out (LOO) or hybrid k-fold cross-validation error estimate for any PCE solution, the same procedure is used: first, the active basis functions are identified using the whole experimental design. Then, the coefficients are recomputed several times using OLS, following the chosen cross-validation framework. This requires solving a linear system of equations k times in the case of k-fold cross-validation. In case of LOO, only one linear system of equations needs to be solved (Blatman and Sudret, 2010a). Furthermore, we can make use of the modification factor of Eq. (6) to compute the hybrid modified LOO error estimate.

As baseline cases, we will also select a solution 1) randomly from a set of generally well-performing methods, and 2) corresponding to the best combination identified in the benchmark of basis adaptivity schemes (Section 3.1).

3 Numerical results

In this benchmark, we compare the performance of various combinations of sparse regression solvers with basis-adaptive schemes. We use the following methods and associated implementations. The sparse solvers (wrapped to fit into our benchmark framework) are:

- Hybrid-LARS: UQLab (Marelli and Sudret, 2019)
- OMP: UQLab (Marelli and Sudret, 2019)
- $\text{SP}_{k=4}$: DOPT_PCE (Diaz et al., 2018; Diaz, 2018)
- SP_{LOO}: own adaptation of Diaz et al. (2018); Diaz (2018)
- BCS: FastLaplace (Babacan et al., 2010; Babacan, 2011)
- SPGL1: SPGL1 (van den Berg and Friedlander, 2008; Van den Berg and Friedlander, 2015)

The basis-adaptive schemes are:

- p&q adaptivity: UQLab (Marelli and Sudret, 2014)
- forward neighbor basis adaptivity: own implementation of the algorithm based on the description by Jakeman et al. (2015)
- anisotropic degree basis adaptivity: own implementation of an algorithm adapted from the basis-adaptive part of BASE-PC (Hampton and Doostan, 2018) (see Section 2.3.3)

To reduce the complexity of our benchmark, we choose Latin hypercube sampling with maximin distance optimization to generate the experimental design (ED) since Lüthen et al. (2020)

demonstrated that the choices of sparse solver and sampling scheme are mostly independent from each other.

We use the following model selection methods:

- For the selection of the hyperparameters of the sparse regression solvers, we use
  - modified OLS-based LOO for the solvers LARS, OMP and SP_{LOO}
  - k-fold CV for the solvers $\text{SP}_{k=4}$, BCS and SPGL1
- The basis adaptivity schemes use the same criterion as the respective solver uses.
- We investigate in Section 3.2 which criterion is suited best for the final model selection.

For our benchmark, we use 11 benchmark models ranging from low-dimensional analytical models to high-dimensional differential equations. All of these models have previously been used as numerical examples for surrogate modeling or reliability analysis. Table 1 provides an overview of the benchmark models. For a more detailed presentation, we refer the interested reader to the respective publications (see column "Reference" of Table 1).

3.1 Basis adaptivity

We benchmark the sparse solvers LARS, OMP, $\text{SP}_{k=4}$, SP_{LOO}, BCS, and SPGL1 combined with the basis-adaptive schemes described in Section 2.3:

1. degree and q-norm (p&q) adaptivity (abbreviation: PQ)
2. forward neighbor basis adaptivity (FN)
3. anisotropic degree basis adaptivity (AD)

As a base case, we include a *static basis* following the rule $P \approx \frac{10}{3}N$ (abbreviation: ST), where we use hyperbolic truncation with $q = 0.5$ for high-dimensional models ($d \geq 20$). The benchmark is performed on all 11 models presented in Table 1. The experimental design is created by Latin hypercube sampling (LHS) with optimized maximin distance. We investigate one “small” and one “large” experimental design size per model (see last column of Table 1). For each model and experimental design size, we repeat the analysis $R = 30$ times to account for the stochasticity of the sampling method. Due to their relatively high computational cost, we omit SPGL1 and anisotropic degree basis adaptivity from the benchmark for high-dimensional models. More details on the settings for the basis adaptivity schemes (e.g., initial basis and investigated degree ranges) can be found in Appendix A.

The aggregated rankings based on the relative MSE are shown in Figs. 2a–2d in the form of stacked bar plots. We analyze the results for low- and high-dimensional models as well as small and large ED sizes separately, resulting in $2 \times 2 = 4$ different cases. The relative ranking of each combination of solver and basis adaptivity scheme is determined on each ED separately.

Table 1: *Overview of the 11 computational models used in our benchmark. Finite element models are marked in italic font, all other models are analytical. The column "Reference" provides the literature in which the models and their input are described in detail. The column "ED sizes" contains the two sizes of experimental design (small and large) used in the basis adaptivity benchmark.*

Model	Dimension	Distributions	Reference	ED sizes (small, large)
Ishigami function	3	uniform	Blatman and Sudret (2011)	50, 150
Undamped oscillator	6	Gaussian	Echard et al. (2013)	60, 120
Borehole function	8	Gaussian, lognormal, uniform	Morris et al. (1993)	100, 250
Damped oscillator	8	lognormal	Dubourg (2011)	150, 350
Wingweight function	10	uniform	Forrester et al. (2008)	100, 250
Truss model	10	lognormal, Gumbel	Blatman and Sudret (2011)	100, 250
Morris function	20	uniform	Blatman and Sudret (2010b)	150, 350
Structural frame model	21	lognormal, Gaussian; dependent input variables	Blatman and Sudret (2010a)	150, 350
2-dim diffusion model	53	Gaussian	Konakli and Sudret (2016)	100, 400
1-dim diffusion model	62	Gaussian	Fajraoui et al. (2017)	100, 400
High-dim. function	100	uniform	UQLab example	400, 1200

This data is aggregated over all repetitions and all models of the respective dimensionality. The ranking considers all combinations of solver and basis adaptivity scheme, i.e., $6 \times 4 = 24$ combinations for the low-dimensional models (Figs. 2a, 2b), and $5 \times 3 = 15$ combinations for the high-dimensional models (Figs. 2c, 2d) and a plot containing aggregated results over all models (Fig. 2e).

The color scale of the stacked bars, ranging from yellow to blue, visualizes how often each combination attained the respective ranking. The triangles in hues of red illustrate how often the respective combination was within a factor of 2, 5, or 10 of the best relative MSE that was obtained by any of the combinations on the same ED. We only show the six combinations of solver and basis adaptivity scheme whose relative MSE was most often within two times the best relative MSE, and sort the combinations according to this criterion (red triangle). (For the full list of combinations, see Figs. 4–7 in the appendix. For boxplots of the results separated by model, see Figs. 8 and 9 in the appendix.)

Comparing the subplots 2a–2d, we observe that the results for small and large ED sizes and low- and high-dimensional models are indeed quite different, which justifies analyzing the results separately. The plots show both which combinations of solver and basis adaptivity scheme attain the smallest relative MSE how often (length of the yellow bar and the position of the red triangle), and how robust the combination is (position of the three triangles), i.e., how often the solution was within a factor of the best solution. We observe that depending on the criterion considered to assess the combinations of solver and basis adaptivity scheme, different combinations turn out to perform best. In the following, we summarize the performance of solver-basis adaptivity combinations with three numbers X-Y-Z, where X denotes the percentage of runs where the respective combination turned out best (i.e., the length of the bright yellow bar), Y denotes the percentage of runs that were within a factor of two of the smallest error on that ED (red triangle), and Z denotes the percentage of runs that were within 1 order of magnitude of the smallest error (light red triangle). The numbers are rounded to integer values. Italic numbers indicate that this is the best value achieved among all combinations. The enumeration tags refer to the panels in Figure 2.

(2a) *Low-dimensional models, small ED*: BCS together with forward neighbor basis adaptivity (*26*-*59*-74) achieves the smallest error more often than any other combination. However, this combination is not the most robust: in $100 - 74 = 26\%$ of runs, its error is more than one magnitude worse than the best error. $\mathrm{SP}_{\mathrm{LOO}}$ together with p&q adaptivity (8-36-*88*) is most robust.

(2b) *Low-dimensional models, large ED*: by far the best combination in all three categories is $\mathrm{SP}_{\mathrm{LOO}}$ together with forward neighbor basis adaptivity (*38*-*64*-*96*).

(2c) *High-dimensional models, small ED*: there are two combinations that outperform the others: BCS with p&q adaptivity (*28*-69-*100*) and BCS with a static basis (2-*74*-*100*).

(2d) *High-dimensional models, large ED*: the two best combinations are $\mathrm{SP}_{k=4}$ with forward

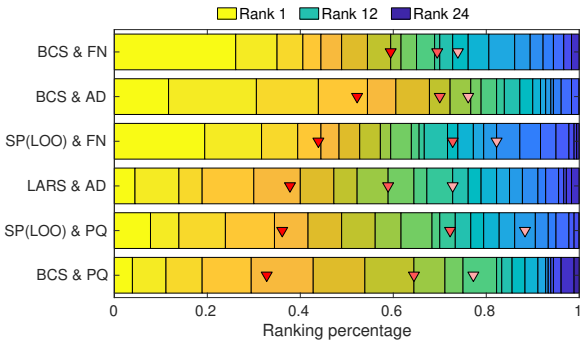

(a) low-dimensional models, small ED

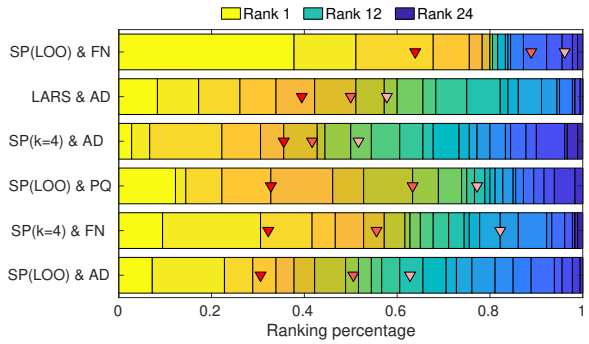

(b) low-dimensional models, large ED

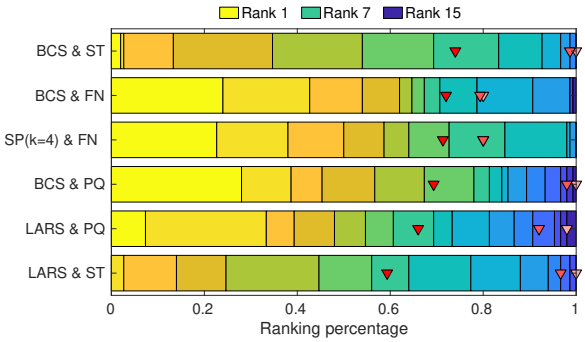

(c) high-dimensional models, small ED

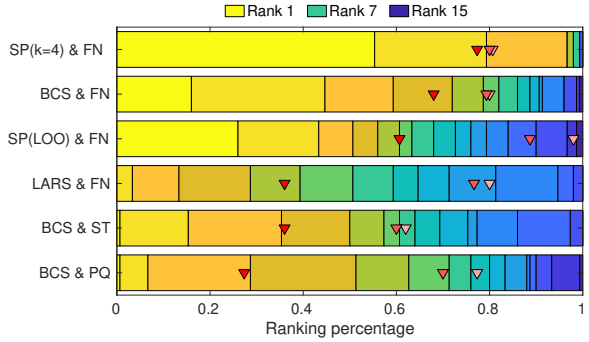

(d) high-dimensional models, large ED

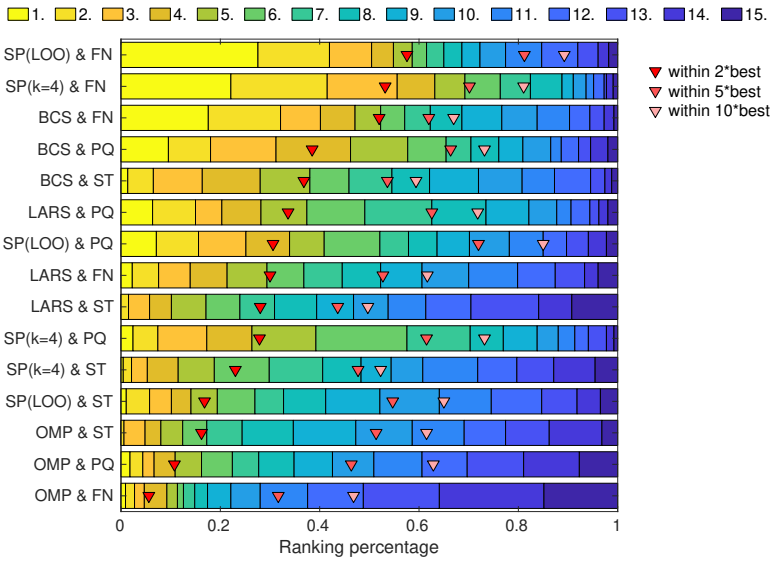

(e) Aggregated results for all models and ED sizes

Figure 2: *Visualization of rankings for the combinations of sparse solvers and basis adaptivity schemes. For each model, each ED size and each replication, the ranking of the combinations is determined based on the relative MSE. The rankings are aggregated for low- and high-dimensional models as well as small and large EDs separately (top) or over all models and ED sizes, respectively (panel 2e). The color scale of the stacked bars, ranging from yellow to blue, visualizes how often each combination attained the respective ranking. The triangles in hues of red denote the percentage of results that were within a factor ($\{2, 5, 10\}$) of the best relative MSE for the specific ED.*

neighbor basis adaptivity (*55*-*77*-81) and SP_{LOO} with forward neighbor basis adaptivity (26-61-*98*).

We observe that from the list of six solvers, only BCS, $\text{SP}_{k=4}$ and SP_{LOO} are found among the best combinations. Considering the best six combinations (based on Y) as in Fig. 2, only LARS is joining the list. OMP does not perform well in any of the cases (see also Appendix, Figs. 4–7). This is likely due to its tendency to severely underestimate the generalization error, which might make the comparison between error estimates of different bases unreliable. Likewise, SPGL1 is never among the best six combinations for low-dimensional models.

Regarding basis adaptivity schemes, the static basis is not among the best six combinations (based on Y) for low-dimensional models. However for high-dimensional models, especially for the small ED case, it is among the six best combinations several times and performs well.

To get a complete picture of solver and basis adaptivity scheme performance, we display in Fig. 2e the relative performance of all combinations of solvers and basis adaptivity schemes, averaged over all models and experimental designs regardless of their dimensionality and size. We exclude combinations involving SPGL1 and anisotropic degree basis adaptivity (AD), which were only tested for low-dimensional models. Therefore, Fig. 2e contains $3 \times 5 = 15$ combinations. We see that SP_{LOO} together with forward neighbor basis adaptivity (*28*-*58*-*89*) performs best in all three categories. $\text{SP}_{k=4}$ together with forward neighbor basis adaptivity (22-53-81) is on the second place in terms of the first two criteria (X and Y). However, SP_{LOO} together with p&q basis adaptivity (7-31-85) is the second-best solver in terms of achieving an error within one order of magnitude of the best error most often (Z). BCS together with any basis adaptivity scheme performs well, while all combinations involving OMP are on the bottom of the list. Combinations with a static basis are found more towards the end of the list, and those with forward neighbor basis adaptivity are found more towards the beginning of the list.

From these plots, we see clearly that there is no single combination of sparse solver and basis adaptivity scheme that always outperforms all others. While SP_{LOO} together with forward neighbor basis adaptivity shows superior performance when averaged over all models and ED sizes, we identify better-performing combinations when we differentiate by model dimension and ED size. In some cases, we are faced with a trade-off between accuracy and robustness: e.g., for high-dimensional models and large EDs, the choice of $\text{SP}_{k=4}$ & FN has a higher probability of yielding a close-to-optimal solution, while the choice of SP_{LOO} & FN has a higher probability of not being too far off from the optimal one. The same holds for low-dimensional models and small EDs for the combinations BCS & FN vs. SP_{LOO} & PQ.

3.2 Automated selection of sparse solver and basis adaptivity scheme

As we saw in the previous section, there is no single best-performing combination of sparse solver and basis adaptivity scheme. In this section, we investigate whether it is possible to select a well-performing combination from a number of candidate combinations using a model selection criterion (*meta-selection*).

For each model, ED size and repetition, the combination of basis adaptivity scheme and sparse solver that minimizes the considered selection index is chosen to be the final meta-model. Due to the performance of the methods in the benchmark in the previous sections, we restrict our investigation to the solvers $\mathrm{SP}_{k=4}$, $\mathrm{SP}_{\mathrm{LOO}}$ and BCS, and to the basis adaptivity schemes

- p&q adaptivity (PQ), forward neighbor adaptivity (FN), and anisotropic degree adaptivity (AD) for low-dimensional models
- static basis (static), p&q adaptivity (PQ), and forward neighbor adaptivity (FN) for high-dimensional models

resulting in 9 possible solutions for each model, ED size and repetition.

We use the following model selection criteria (see also Section 2.4):

1. the oracle solution, i.e, the smallest relative MSE attained among the 9 combinations on each ED realization, as a lower bound. Of course, this information is not available in practice.
2. the criterion used for basis and hyperparameter selection by the respective solver (see Section 2.1)
3. hybrid LOO, computed by OLS on the active basis functions only
4. hybrid modified LOO, computed by OLS on the active basis functions only, and using the correction factor from Eq. (6)
5. hybrid 10-fold cross-validation error, computed by OLS on the active basis functions only
6. A fixed rule dependent on dimensionality and ED size, according to the findings in Section 3.1, choosing the solver that was ranked first most often (bright yellow bar):
   - low-dimensional models, small ED: BCS & FN
   - low-dimensional models, large ED: $\mathrm{SP}_{\mathrm{LOO}}$ & FN
   - high-dimensional models, small ED: BCS & PQ
   - high-dimensional models, large ED: $\mathrm{SP}_{k=4}$ & FN
7. A randomly picked combination of solver and basis adaptivity scheme as upper bound: any sensible model selection criterion must perform better than this.

The results are presented in Figure 3. Note that we do not display which sparse solver and basis adaptivity scheme was chosen – we only show how close the chosen solution comes to the best possible solution.

- By construction, the oracle selection performs best in all cases.
- The random selection is by far the worst selection criterion, which shows that meta-selection provides a statistically significant improvement over random selection.

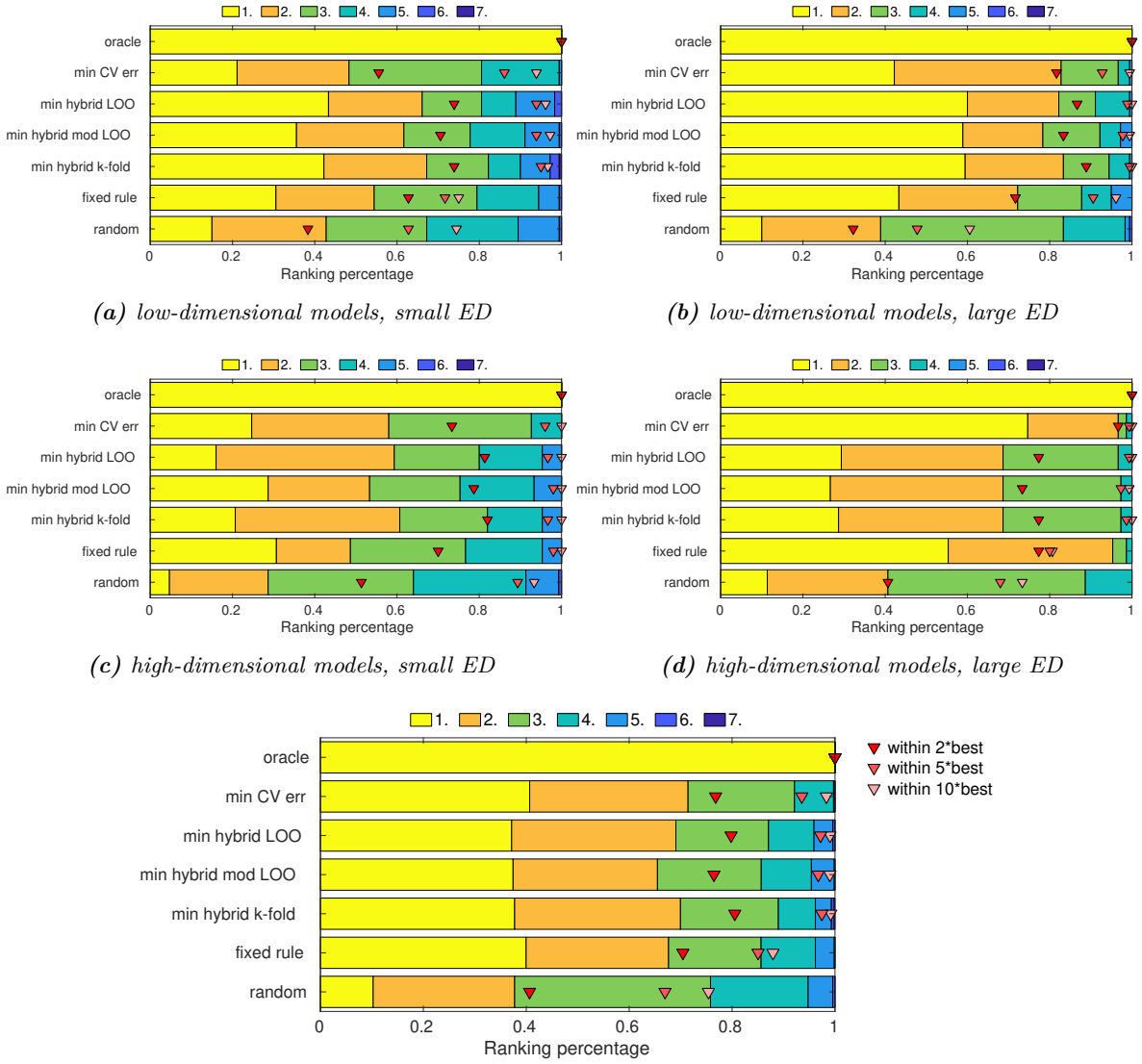

(a) low-dimensional models, small ED

(b) low-dimensional models, large ED

(c) high-dimensional models, small ED

(d) high-dimensional models, large ED

(e) All dimensionalities and ED sizes in one

Figure 3: *Testing different model selection strategies. As before, the stacked bar plot visualizes the percentage of runs where the respective strategy ranked first, second, etc., among the seven selection strategies. The triangles in hues of red illustrate how many of the runs yielded a result that was within a factor of* $\{2, 5, 10\}$ *of the best error.*

- The fixed rule is overall less robust than the hybrid CV selection criteria (light red triangle). Furthermore, it does not find the best or second-best solution more often than the hybrid CV selection criteria.

- The criterion used for basis and hyperparameter selection, i.e., k-fold CV for $\mathrm{SP}_{k=4}$ and BCS, and LOO for $\mathrm{SP}_{\mathrm{LOO}}$, performs slightly worse than the three hybrid selection criteria – except for high-dimensional models with a large ED, for which this criterion performs best by a large margin (Fig. 3d). Overall, this results in an almost identical performance of this and the hybrid criteria when all models and ED sizes are combined (Fig. 3e). The relatively poor performance of this selection criterion for low-dimensional models and small experimental designs might be explained by selection bias: since the criterion was already used twice for selection, it is likely that it underestimates the generalization error. Another reason might be that different solvers use different criteria which might not be comparable among each other (inconsistency).

- The three other model selection criteria hybrid LOO, hybrid modified LOO, and hybrid 10-fold CV perform almost identically, especially when averaging the results over all models and ED sizes. Note that all three attain in almost all cases an error which is within one order of magnitude of the oracle solution, which is significantly better than any fixed combination of methods (compare Figs. 2e and 3e).

We conclude that meta-selection, i.e., using cross-validation to choose a PCE solution from a number of candidate solutions computed with different methods on the same experimental design, can achieve more robust and slightly more accurate results than a fixed rule on which combination of solver and basis adaptivity scheme to use, even if this rule is based on a thorough benchmark such as the one in Section 3.1.

4 Conclusion and discussion

We investigated several approaches for computing sparse PCE with the goal of surrogate modeling, using the relative mean squared error on a validation set as the main performance metric. In particular, we studied the performance of combinations of basis adaptivity schemes and sparse solvers in order to identify combinations that yield the smallest generalization error. Our investigations are based on 11 analytical and numerical benchmark models of varying input dimension and complexity, representative of a wide range of engineering problems. We considered the sparse solvers least angle regression (LARS), orthogonal matching pursuit (OMP), subspace pursuit based on k-fold cross-validation ($\mathrm{SP}_{k=4}$), subspace pursuit based on LOO ($\mathrm{SP}_{\mathrm{LOO}}$), Bayesian compressive sensing/FastLaplace (BCS), and spectral projected gradient-ℓ^1 (SPGL1). The basis adaptivity schemes we compared were a fixed basis truncation scheme following the rule $N \approx \frac{10}{3}P$, degree- and q-norm adaptivity, forward neighbor basis adaptivity, and anisotropic degree basis adaptivity. We made a distinction between four cases, namely low- and high-dimensional models as well as small and large experimental design sizes.

The benchmark revealed that the difference in generalization error between different combinations of methods can be large, even more than an order of magnitude. In each of the four cases, we were able to find combinations that generally perform well. These combinations always involved the solvers $\mathrm{SP}_{\mathrm{LOO}}$, $\mathrm{SP}_{k=4}$, or BCS, but never SPGL1 or OMP. For the basis-adaptive schemes, the picture is less clear, except that the static basis (i.e., no basis adaptivity) was in nearly all cases outperformed by basis-adaptive schemes. There is no combination of solver and basis-adaptive scheme that was consistently best across all models and experimental design sizes, although averaging over all four cases, $\mathrm{SP}_{\mathrm{LOO}}$ together with forward neighbor basis adaptivity outperformed all other combinations.

Since no clear best combination of solver and basis adaptivity scheme emerged, we introduced an automatic meta-selection step. Based on a suitable error estimate, meta-selection chooses one PCE solution out of several candidate solutions computed by various combinations of solvers and basis adaptivity schemes. We found that meta-selection using any hybrid cross-validation error estimate performs better than the fixed rules obtained from the basis adaptivity benchmark both in terms of attained relative MSE and robustness, and far better than a random selection of solver and basis adaptivity scheme. An additional advantage of meta-selection is that it is automatic and independent of model dimension or size of the available experimental design, unlike the proposed fixed rules, which rely on the somewhat arbitrary (albeit simple) classification we applied (low/high dimension and small/large experimental design).

These findings demonstrate that when building a sparse PCE for an expensive black-box computational model, it is worth it to carefully select a sparse solver, and to apply a basis-adaptive scheme, because the difference in relative MSE between different combinations of methods on the same experimental design can be larger than one order of magnitude. While we could identify a number of methods that generally perform well, and others that should be avoided, a superior strategy is to compute several PCE solutions and perform a final model selection using one of the presented hybrid cross-validation error estimators.

Further research is needed to investigate the use of true cross-validation for meta-selection instead of the hybrid estimates which we used here. Also, it might be possible to identify other problem characteristics besides its dimension and the size of the available experimental design to guide the choice of methods in the sparse PCE framework. A promising class of methods combines basis adaptivity with the sequential enrichment of the experimental design, adapted to the current candidate or active basis (Fajraoui et al., 2017; Diaz et al., 2018; Hampton and Doostan, 2018), which might be able to further improve on the results obtained here.

Acknowledgments

We thank John Jakeman (Sandia National Laboratories), Negin Alemazkoor (University of Massachusetts Dartmouth), Hadi Meidani (University of Illinois at Urbana-Champaign), and Jerrad Hampton (University of Colorado Boulder) for generously providing their code and explanations. We thank John Jakeman for his useful hints to relevant literature on basis adaptivity.

References

Abbiati, G., S. Marelli, N. Tsokanas, B. Sudret, and B. Stojadinovic (2021). A global sensitivity analysis framework for hybrid simulation. *Mechanical Systems and Signal Processing 146*, 106997.

Adams, B. M., L. E. Bauman, W. J. Bohnhoff, K. R. Dalbey, M. S. Ebeida, J. P. Eddy, M. S. Eldred, P. D. Hough, K. T. Hu, J. D. Jakeman, J. A. Stephens, L. P. Swiler, D. M. Vigil, , and T. M. Wildey (2014). *Dakota, A Multilevel Parallel Object-Oriented Framework for Design Optimization, Parameter Estimation, Uncertainty Quantification, and Sensitivity Analysis: Version 6.0 User's Manual*. Sandia National Laboratories. Technical Report SAND2014-4633 (Updated November 2015 (Version 6.3)).

Alemazkoor, N. and H. Meidani (2017). Divide and conquer: An incremental sparsity promoting compressive sampling approach for polynomial chaos expansions. *Comput. Methods Appl. Mech. Engrg. 318*, 937–956.

Babacan, D. (2011). MATLAB code for the TIP 2009 paper "Bayesian Compressive Sensing using Laplace Priors". `http://www.dbabacan.info/software.html`. [Online; accessed 28-August-2019].

Babacan, S., R. Molina, and A. Katsaggelos (2010). Bayesian compressive sensing using Laplace priors. *IEEE Trans. Image Process. 19*(1), 53–63.

Blatman, G. and B. Sudret (2009). Anisotropic parcimonious polynomial chaos expansions based on the sparsity-of-effects principle. In H. Furuta, D. Frangopol, and M. Shinozuka (Eds.), *Proc. 10th Int. Conf. Struct. Safety and Reliability (ICOSSAR'2009), Osaka, Japan.*

Blatman, G. and B. Sudret (2010a). An adaptive algorithm to build up sparse polynomial chaos expansions for stochastic finite element analysis. *Prob. Eng. Mech. 25*, 183–197.

Blatman, G. and B. Sudret (2010b). Efficient computation of global sensitivity indices using sparse polynomial chaos expansions. *Reliab. Eng. Sys. Safety 95*, 1216–1229.

Blatman, G. and B. Sudret (2011). Adaptive sparse polynomial chaos expansion based on Least Angle Regression. *J. Comput. Phys 230*, 2345–2367.

Bruckstein, A. M., D. L. Donoho, and M. Elad (2009). From sparse solutions of systems of equations to sparse modeling of signals and images. *SIAM review 51*(1), 34–81.

Candès, E. J. and Y. Plan (2011). A probabilistic and RIPless theory of compressed sensing. *IEEE Trans. Inform. Theory 57*(11), 7235–7254.

Candès, E. J. and M. B. Wakin (2008). An introduction to compressive sampling: A sensing/sampling paradigm that goes against the common knowledge in data acquisition. *IEEE Signal Process. Mag. 25*(2), 21–30.

Chapelle, O., V. Vapnik, and Y. Bengio (2002). Model selection for small sample regression. *Machine Learning 48*(1), 9–23.

Chatterjee, T., S. Chakraborty, and R. Chowdhury (2019). A critical review of surrogate assisted robust design optimization. *Arch. Comput. Method. E. 26*(1), 245–274.

Diaz, P. (2018). DOPT_PCE. `https://github.com/CU-UQ/DOPT_PCE`. [Online; accessed 14-May-2020].

Diaz, P., A. Doostan, and J. Hampton (2018). Sparse polynomial chaos expansions via compressed sensing and D-optimal design. *Comput. Methods Appl. Mech. Engrg. 336*, 640–666.

Doostan, A. and H. Owhadi (2011). A non-adapted sparse approximation of PDEs with stochastic inputs. *J. Comput. Phys. 230*(8), 3015–3034.

Dubourg, V. (2011). *Adaptive surrogate models for reliability analysis and reliability-based design optimization*. Ph. D. thesis, Université Blaise Pascal, Clermont-Ferrand, France.

Echard, B., N. Gayton, M. Lemaire, and N. Relun (2013). A combined importance sampling and Kriging reliability method for small failure probabilities with time-demanding numerical models. *Reliab. Eng. Syst. Safety 111*, 232–240.

Efron, B., T. Hastie, I. Johnstone, and R. Tibshirani (2004). Least angle regression. *Ann. Stat. 32*, 407–499.

Ernst, O., A. Mugler, H.-J. Starkloff, and E. Ullmann (2012). On the convergence of generalized polynomial chaos expansions. *ESAIM: Math. Model. Numer. Anal. 46*(02), 317–339.

Fajraoui, N., S. Marelli, and B. Sudret (2017). Sequential design of experiment for sparse polynomial chaos expansions. *SIAM/ASA J. Unc. Quant. 5*(1), 1061–1085.

Forrester, A., A. Sobester, and A. Keane (2008). *Engineering design via surrogate modelling: a practical guide*. Wiley.

Gerstner, T. and M. Griebel (2003). Dimension-adaptive tensor-product quadrature. *Computing 71*, 65–87.

Guo, X., D. Dias, and Q. Pan (2019). Probabilistic stability analysis of an embankment dam considering soil spatial variability. *Comput. Geotech. 113*, 103093.

Hampton, J. and A. Doostan (2017). BASE_PC. `https://github.com/CU-UQ/BASE_PC`. [Online; accessed 14-May-2020].

Hampton, J. and A. Doostan (2018). Basis adaptive sample efficient polynomial chaos (BASE-PC). *J. Comput. Phys. 371*, 20–49.

Harari-Ardebili, M. and B. Sudret (2020). Polynomial chaos expansion for uncertainty quantification of dam engineering problems. *Engineering Structures 203*.

Jakeman, J. D., M. S. Eldred, and K. Sargsyan (2015). Enhancing ℓ_1-minimization estimates of polynomial chaos expansions using basis selection. *J. Comput. Phys. 289*, 18–34.

Konakli, K. and B. Sudret (2016). Global sensitivity analysis using low-rank tensor approximations. *Reliab. Eng. Sys. Safety 156*, 64–83.

Le Gratiet, L., S. Marelli, and B. Sudret (2017). *Metamodel-based sensitivity analysis: polynomial chaos expansions and Gaussian processes*, Chapter 8, Handbook on Uncertainty Quantification (Ghanem, R. and Higdon, D. and Owhadi, H. (Eds.). Springer.

Loukrezis, D. and H. De Gersem (2019). Adaptive sparse polynomial chaos expansions via Leja interpolation. *arXiv preprint arXiv:1911.08312*.

Lüthen, N., S. Marelli, and B. Sudret (2020). Sparse polynomial chaos expansions: Literature survey and benchmark. *SIAM/ASA J. Unc. Quant.*. (submitted).

Mai, C. V. and B. Sudret (2015). Hierarchical adaptive polynomial chaos expansions. In M. Papadrakakis, V. Papadopoulos, and G. Stefanou (Eds.), *1st Int. Conf. on Uncertainty Quantification in Computational Sciences and Engineering (UNCECOMP)*, Creta, Greece.

Marelli, S. and B. Sudret (2014). UQLab: A framework for uncertainty quantification in Matlab. In *Vulnerability, Uncertainty, and Risk (Proc. 2nd Int. Conf. on Vulnerability, Risk Analysis and Management (ICVRAM2014), Liverpool, United Kingdom)*, pp. 2554–2563.

Marelli, S. and B. Sudret (2019). UQLab user manual – Polynomial chaos expansions. Technical report, Chair of Risk, Safety and Uncertainty Quantification, ETH Zurich, Switzerland. Report# UQLab-V1.3-104.

Morris, M. D., T. J. Mitchell, and D. Ylvisaker (1993). Bayesian design and analysis of computer experiments: use of derivatives in surface prediction. *Technometrics 35*, 243–255.

Narayan, A. and J. D. Jakeman (2014). Adaptive Leja sparse grid constructions for stochastic collocation and high-dimensional approximation. *SIAM Journal on Scientific Computing 36*(6), A2952–A2983.

Pati, Y. C., R. Rezaiifar, and P. S. Krishnaprasad (1993). Orthogonal matching pursuit: Recursive function approximation with applications to wavelet decomposition. In *Proc. of 27th Asilomar Conf. on signals, systems and computers*, pp. 40–44. IEEE.

Slot, R., J. D. Sorensen, B. Sudret, L. Svenningsen, and M. Thogersen (2020). Surrogate model uncertainty in wind turbine reliability assessment. *Renewable Energy 151*, 1150–1162.

Sudret, B. (2008). Global sensitivity analysis using polynomial chaos expansions. *Reliab. Eng. Sys. Safety 93*, 964–979.

Thapa, M., S. B. Mulani, and R. W. Walters (2020). Adaptive weighted least-squares polynomial chaos expansion with basis adaptivity and sequential adaptive sampling. *Comput. Meth. Appl. Mech. Eng. 360*, 112759.

van den Berg, E. and M. P. Friedlander (2008). Probing the Pareto frontier for basis pursuit solutions. *SIAM J. Sci. Comput. 31*(2), 890–912.

Van den Berg, E. and M. P. Friedlander (2015). SPGL1 - A Matlab solver for sparse optimization. `https://friedlander.io/software/spgl1/`. [Online; accessed 28-August-2019].

Vapnik, V. N. (1995). *The Nature of Statistical Learning Theory*. Springer-Verlag, New York.

Xiu, D. and G. E. Karniadakis (2002). The Wiener-Askey polynomial chaos for stochastic differential equations. *SIAM J. Sci. Comput. 24*(2), 619–644.

A Details on the settings for the basis adaptivity schemes in the benchmark

In Table 2, we list the basis adaptivity settings for each of the 11 models in our benchmark.

- The rule for the static basis (ST) is to choose a total-degree basis with p so that the number of basis functions P is closest to $\frac{10}{3}N$, where N is the number of ED points. Here, for low-dimensional models, the q-norm is chosen as $q = 1$, while for high-dimensional models, we use $q = 0.5$.
- For degree and q-norm basis adaptivity (PQ), we choose the ranges for degree and q-norm as large as possible while still keeping the number of basis functions computationally manageable (rule of thumb $\lesssim 10^4$).
- For forward neighbor degree adaptivity (FN), the degree of the initial basis is chosen so that the size of the basis is closest to $10N$ (as recommended in (Jakeman et al., 2015)), while we set the q-norm to the maximum of the q-norm-range for PQ basis adaptivity.
- Finally, for anisotropic degree basis adaptivity, which is only used for low-dimensional models, we use $q = 1$ and $p = \lceil \frac{p_{\max}}{2} \rceil$, where $p_{\max}$ is the maximum of the degree range for PQ basis adaptivity.

B Additional results

B.1 Full plots of rankings

In Figs. 4-7, we display the aggregated results for all combinations of solvers and sampling schemes (while in Section 3.1, we only displayed the six best combinations sorted according to how often they achieved an error within two times the best relMSE (red triangle). For a detailed description of how to read this plot, we refer to Section 3.1.

B.2 Basis adaptivity benchmark: raw data

Figs. 8 and 9 show the raw data of the basis adaptivity benchmark: for each model and ED size, we display the boxplots of resulting relative MSE for each combination of sparse solver and basis-adaptive scheme.

Table 2: *Details on the initial bases and degree and q-norm ranges for the various basis adaptivity schemes*

Model	dim d	static basis	PQ range	FN initial	AD initial
Ishigami function	3	$p = 8$ (small ED) / $p = 12$ (large), $q = 1$	$p \in [1, \ldots, 25]$, $q \in [0.5, 0.6, \ldots, 1]$	$p = 12$ (small ED) / $p = 19$ (large)	$p = 13$
Undamped oscillator	6	$p = 4$ / $p = 4$, $q = 1$	$p \in [1, \ldots, 10]$, $q \in [0.5, 0.6, \ldots, 1]$	$p = 5$ / $p = 6$	$p = 5$
Borehole function	8	$p = 4$ / $p = 4$, $q = 1$	$p \in [1, \ldots, 10]$, $q \in [0.5, 0.6, \ldots, 1]$	$p = 5$ / $p = 6$	$p = 5$
Damped oscillator	8	$p = 4$ / $p = 5$, $q = 1$	$p \in [1, \ldots, 7]$, $q \in [0.5, 0.6, \ldots, 1]$	$p = 5$ / $p = 6$	$p = 4$
Wingweight function	10	$p = 3$ / $p = 4$, $q = 1$	$p \in [1, \ldots, 7]$, $q \in [0.5, 0.6, \ldots, 1]$	$p = 4$ / $p = 5$	$p = 4$
Truss model	10	$p = 3$ / $p = 4$, $q = 1$	$p \in [1, \ldots, 6]$, $q \in [0.5, 0.6, \ldots, 1]$	$p = 4$ / $p = 5$	$p = 3$
Morris function	20	$p = 6$ / $p = 8$, $q = 0.5$	$p \in [1, \ldots, 8]$, $q \in [0.4, 0.5, 0.6]$	$p = 6$ / $p = 8$, $q = 0.6$	–
Structural frame model	21	$p = 5$ / $p = 8$, $q = 0.5$	$p \in [1, \ldots, 8]$, $q \in [0.4, 0.5, 0.6]$	$p = 6$ / $p = 8$, $q = 0.6$	–
2-dim diffusion model	53	$p = 3$ / $p = 4$, $q = 0.5$	$p \in [1, \ldots, 6]$, $q \in [0.4, 0.5, 0.6]$	$p = 4$ / $p = 5$, $q = 0.6$	–
1-dim diffusion model	62	$p = 3$ / $p = 4$, $q = 0.5$	$p \in [1, \ldots, 5]$, $q \in [0.4, 0.5, 0.6]$	$p = 3$ / $p = 4$, $q = 0.6$	–
High-dim. function	100	$p = 3$ / $p = 4$, $q = 0.5$	$p \in [1, \ldots, 5]$, $q = 0.5$	$p = 4$ / $p = 5$, $q = 0.5$	–

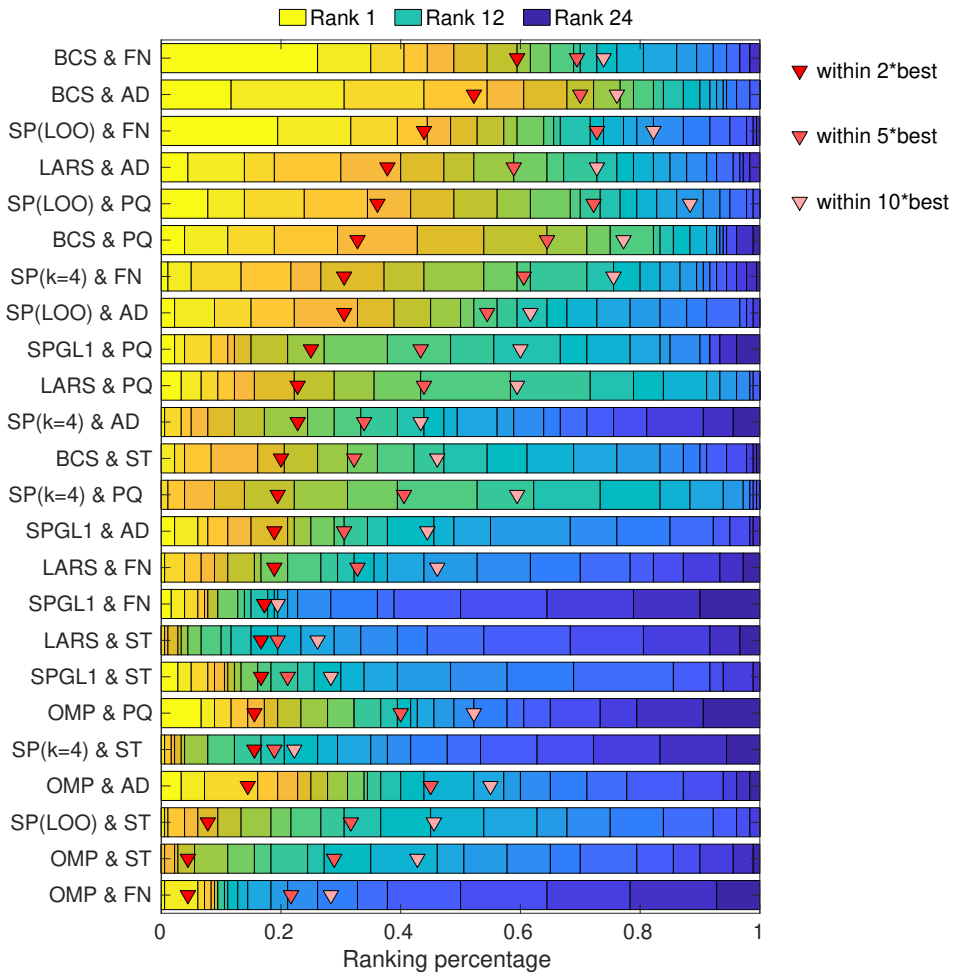

Figure 4: Small ED sizes. *Aggregated results for* ***low-dim*** *models.*

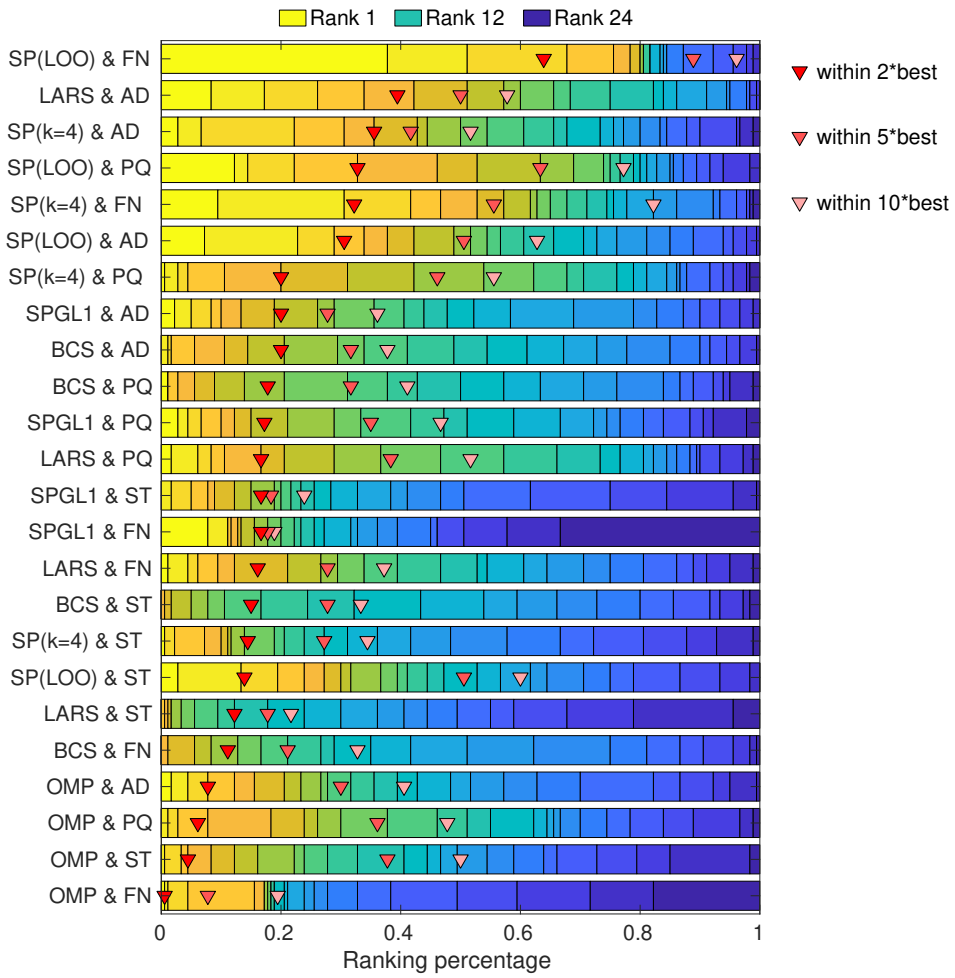

Figure 5: Large ED sizes. *Aggregated results for* ***low-dim*** *models.*

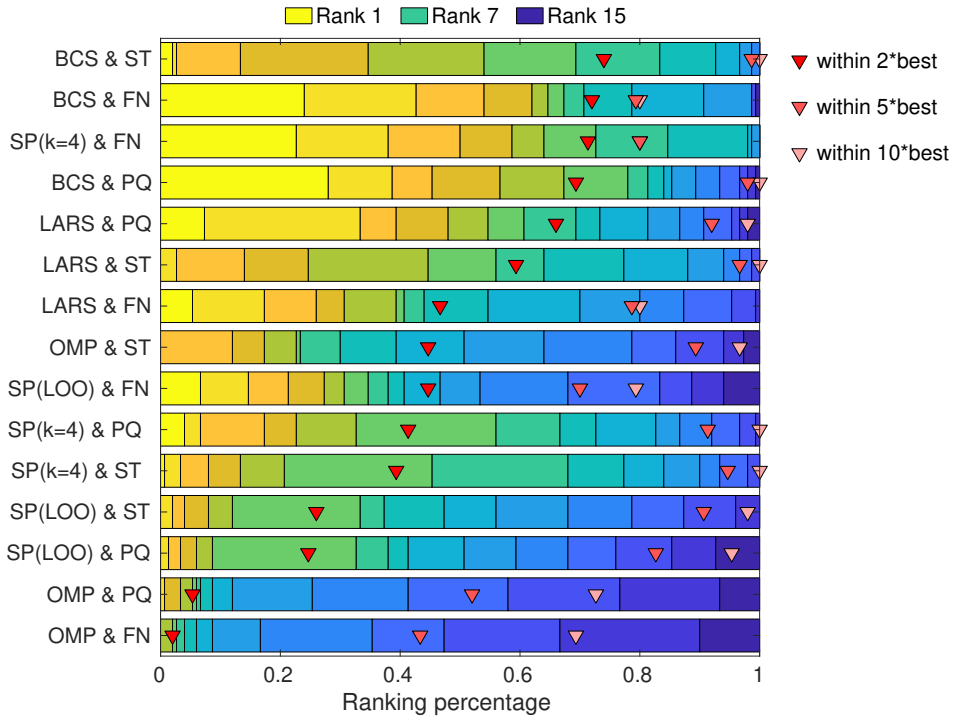

Figure 6: Small ED sizes. *Aggregated results for* ***high-dim*** *models.*

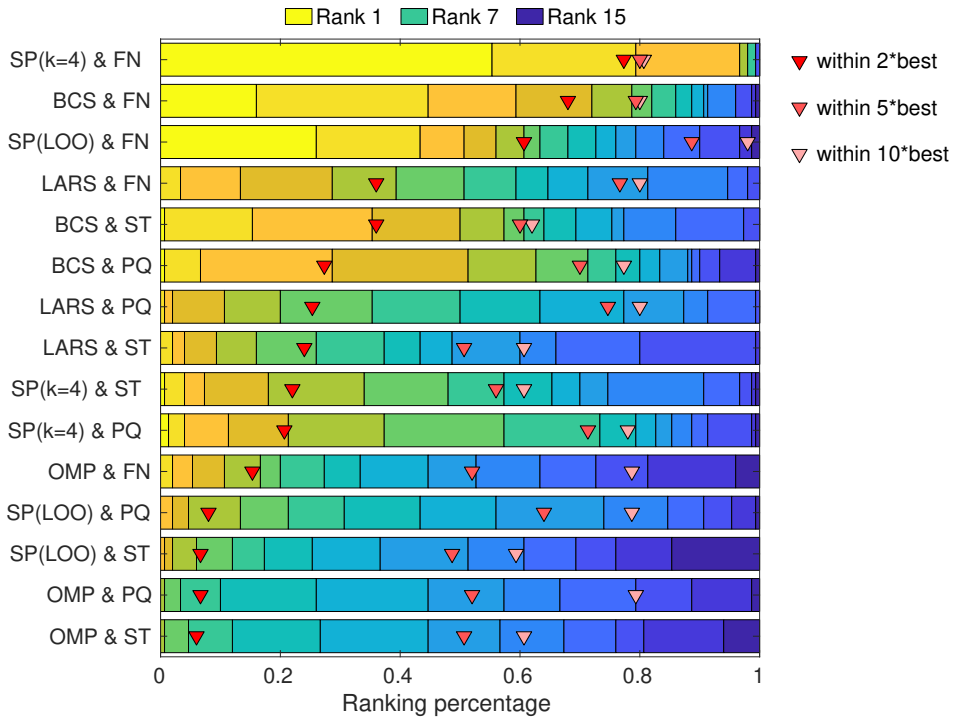

Figure 7: *Aggregated results for* ***high-dim*** *models.* ***Large ED sizes.***

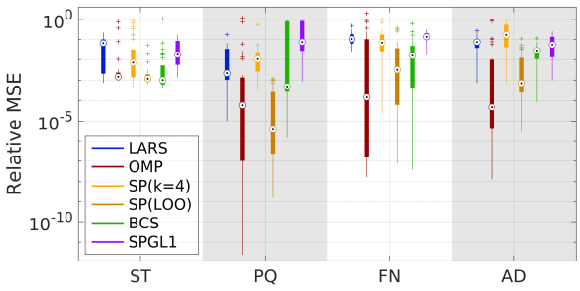

(a) Ishigami function, $N = 50$

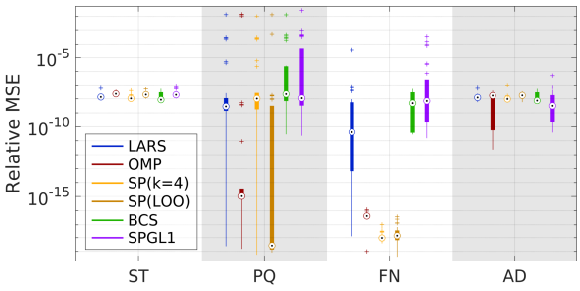

(b) Ishigami function, $N = 150$

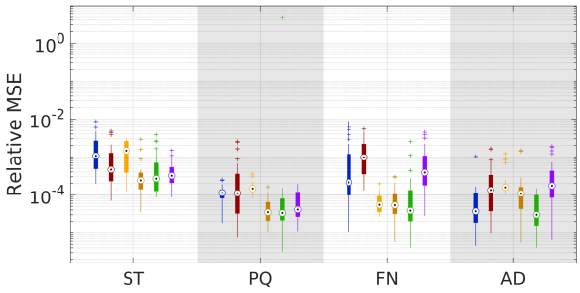

(c) Undamped oscillator, $N = 60$

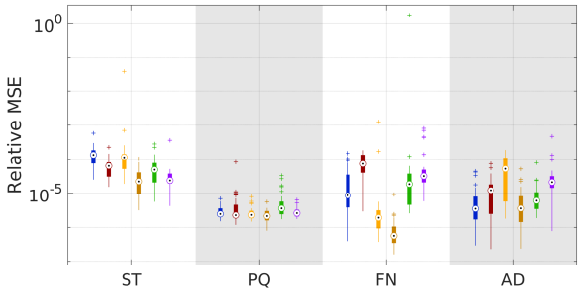

(d) Undamped oscillator, $N = 120$

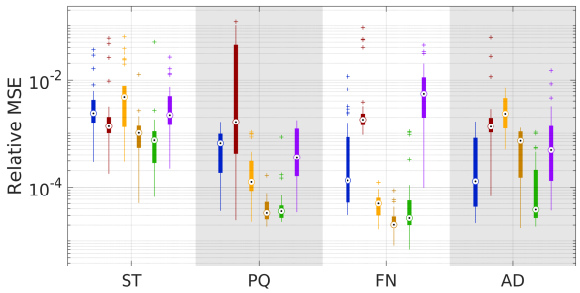

(e) Borehole function, $N = 100$

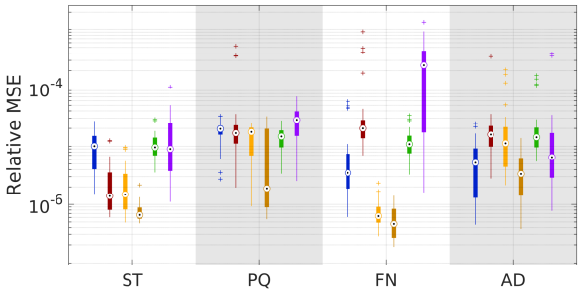

(f) Borehole function, $N = 250$

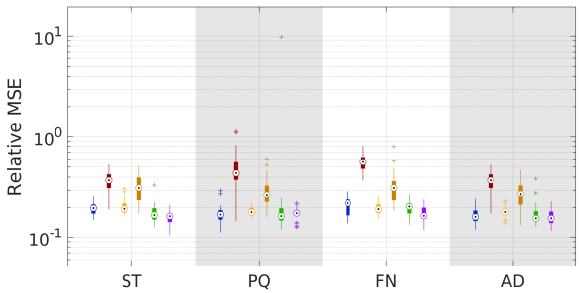

(g) Damped oscillator, $N = 150$

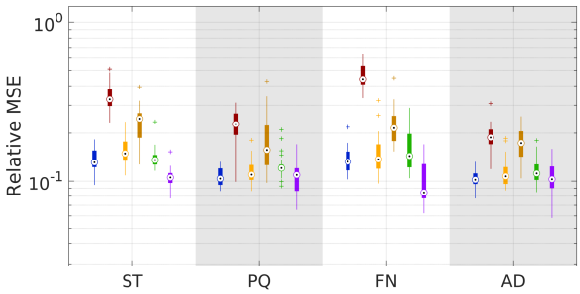

(h) Damped oscillator, $N = 350$

Figure 8: *Comparison of different basis adaptivity schemes.* ***Low-dim models****. Left: small ED; right: large ED. Different colors denote different solvers (LARS, OMP, $SP_{k=4}$, SP_{LOO}, BCS and SPGL1). Continued in next figure.*

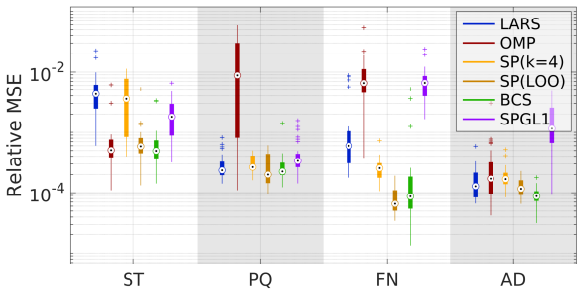

(i) Truss model, $N = 100$

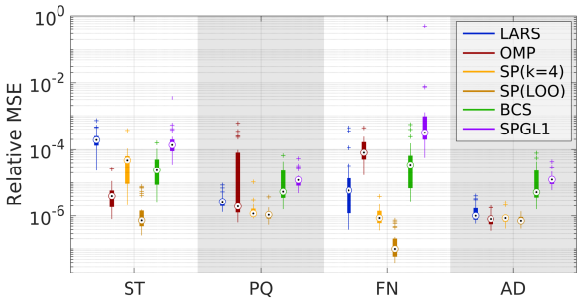

(j) Truss model, $N = 250$

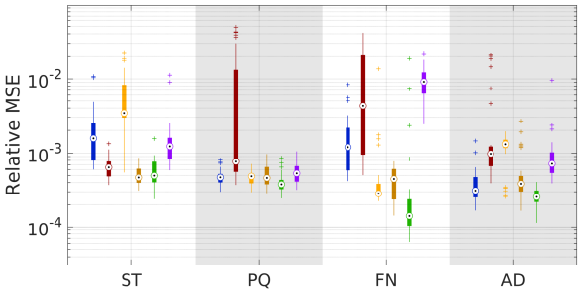

(k) Wingweight function, $N = 100$

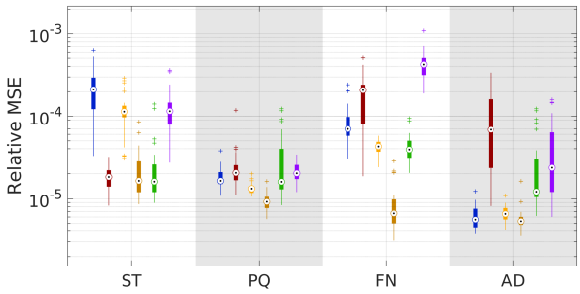

(l) Wingweight function, $N = 250$

Figure 8: *Continued. Comparison of different basis adaptivity schemes.* ***Low-dim models****. Left: small ED; right: large ED. Different colors denote different solvers (LARS, OMP, $SP_{k=4}$, SP_{LOO}, BCS and SPGL1).*

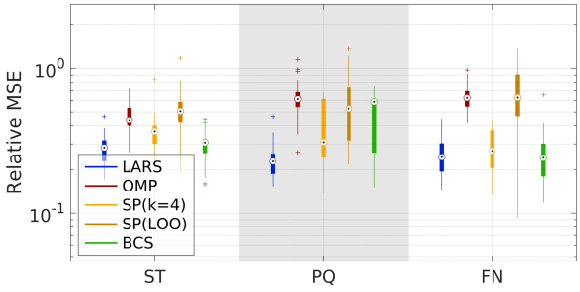

(a) Morris function, $N = 150$

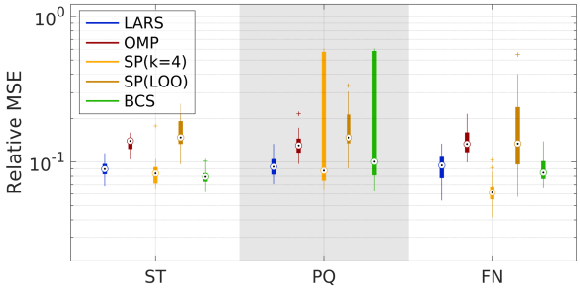

(b) Morris function, $N = 350$

Figure 9: *Comparison of different basis adaptivity schemes.* ***High-dim models****. Left: small ED; right: large ED. Different colors denote different solvers (LARS, OMP, $SP_{k=4}$, SP_{LOO}, and BCS).*

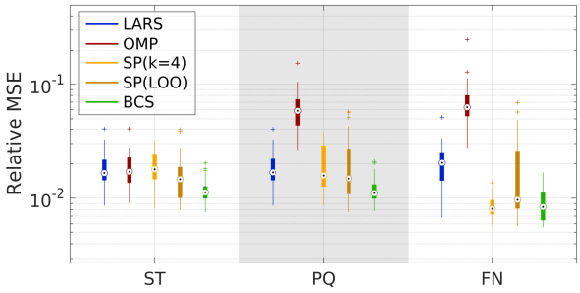

(c) Structural frame, $N = 150$

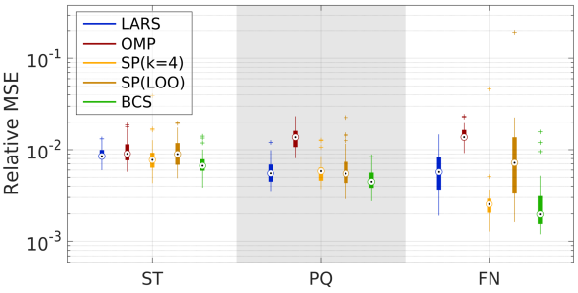

(d) Structural frame, $N = 350$

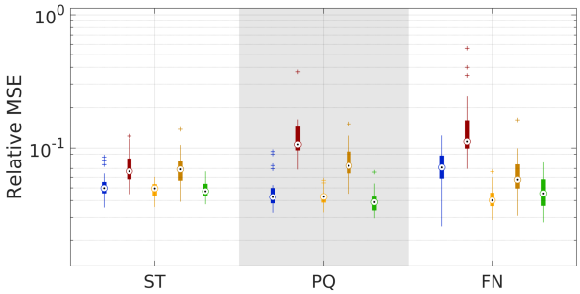

(e) Diffusion 2D, $N = 100$

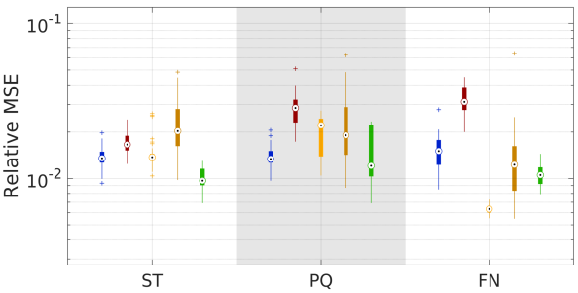

(f) Diffusion 2D, $N = 400$

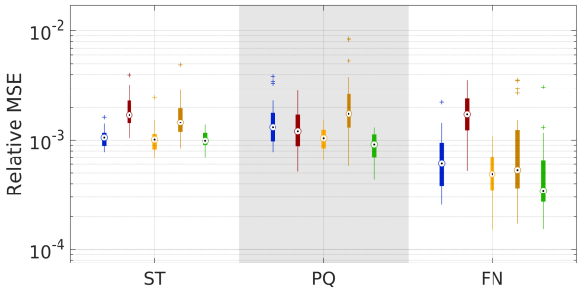

(g) Diffusion 1D, $N = 100$

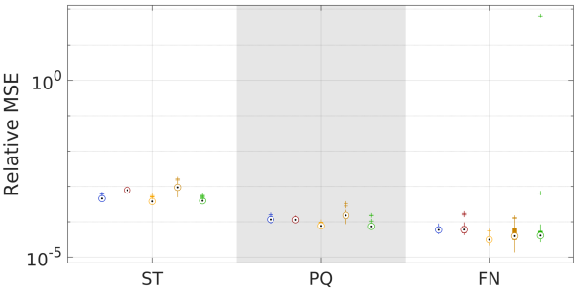

(h) Diffusion 1D, $N = 400$

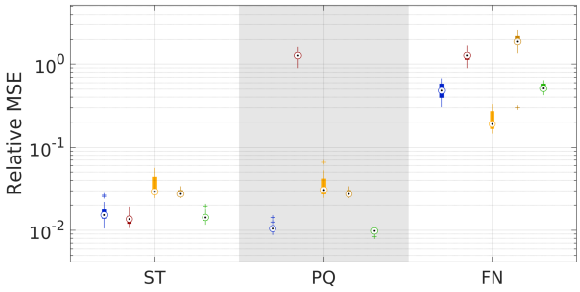

(i) High-dim function, $N = 400$

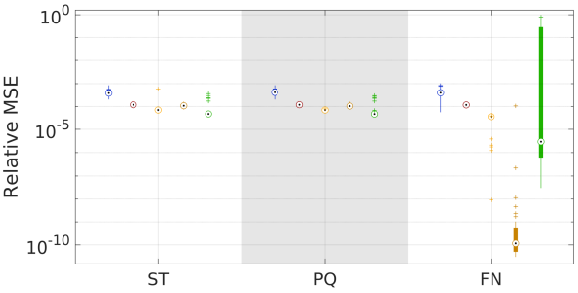

(j) High-dim function, $N = 1200$

Figure 9: *Continued. Comparison of different basis adaptivity schemes.* ***High-dim models****. Left: small ED; right: large ED. Different colors denote different solvers (LARS, OMP, $SP_{k=4}$, SP_{LOO}, and BCS).*